2014

FINAL REPORT OF A SHORT TERM SCIENTIFIC MISSION
COST Action TU1304


Dr Hassan Hemida

Dr Anina Šarkić

[Wind tunnel tests--air flow around buildings]

This is the final report of the Short Term Scientific Mission as part of the COST ACTION TU1304.

Table of contents

1 Background

1.1 Members of the Scientific Mission

The members of this Short Term Scientific Mission are:

1. Dr Anina Šarkić from the Institute of Numerical Analyses and the Theory of Structures, University of Belgrade, Serbia
2. Dr Hassan Hemida from the School of Civil Engineering, University of Birmingham, UK.

1.2 Host Institution

The mission has been undertaken at the Lab of Prof Rüdiger Höffer the Head of Windingenieurwesen und Strömungsmechanik, Faculty for Civil and Environmental Engineering, Ruhr-University Bochum, Germany.

1.3 Mission

The main aim of the STSM was to conduct wind tunnel experiments to investigate the flow around building for the possibility of harvesting wind energy from the above roof flow in built environment. The programme consisted of measuring the velocity in the above roof flow and the surface pressure on a number of building shapes and configurations. These include:

1. A high-rise building with a flat roof.
2. A high-rise building with a tilted roof.
3. A low-rise building with a tilted roof.
4. An industrial building with a tilted roof.

All of the previous building shapes were investigated in isolations considering different angles of flow attack. In addition to the above, the interference effects of the following building configurations were also investigated:

5. Four buildings of the same shape of the high-rise building were places around it.
6. Four buildings of the same shape of the high-rise building were placed around the tilted shape high-rise building.
7. Four buildings of the same shape of the low-rise building were placed around it.

The velocities above the roof of previous building shapes at different heights were measured. Also the surface pressures on the roof and on one or two rings, depending on the building shape, at certain heights from the ground were measured. The STSM provided considerable amount of valuable data for CFD validation. The CFD calculations will be performed after the STSM.

1.4 Time of the mission

The mission started on the 2nd November 2014 and ended on 12 November 2014.

2 Building Shapes

Four different building shapes were used in this work.

2.1 High-rise building with flat roof

The building model mounted in the wind tunnel is shown in Figure 1(a). A 1:300 scale model has height to width ratio of 3:1, as shown in Figure 1(b).

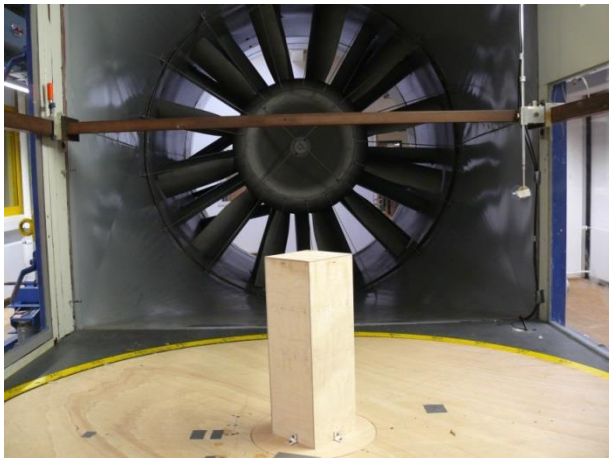

(a)

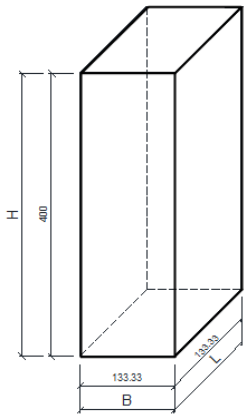

(b)

Figure 1 (a) High-rise building with flat roof mounted in the wind tunnel (b) dimensions of the high-rise model

2.2 High-rise building with tilted roof

The high-rise building with tilted roof is similar in size to the one with flat roof while the roof is tilted as shown in Figure 2.

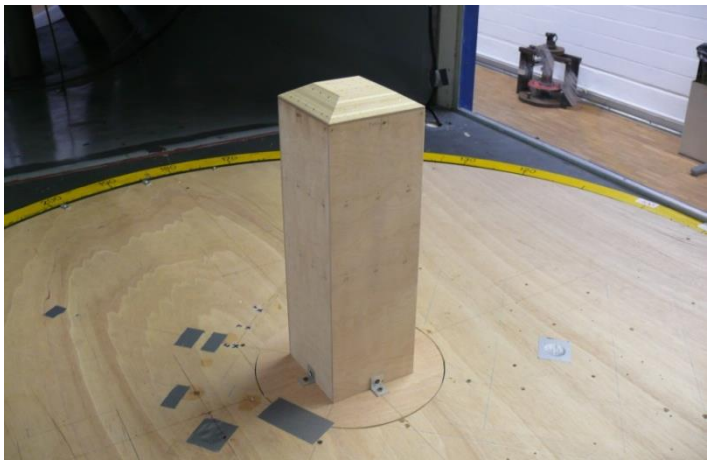

(a)

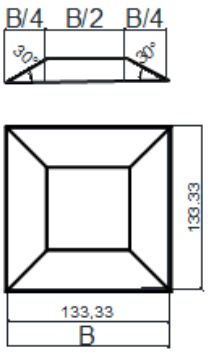

(b)

Figure 2 (a) High-rise building with tilted roof mounted in the wind tunnel, (b) dimensions of the tilted roof model

2.3 Low-rise building with tilted roof

The low-rise building with a house-like shape of scale 1:75 mounted in the wind tunnel is shown in Figure 3 (a). Dimensions of the building are shown in Figure 3 (b).

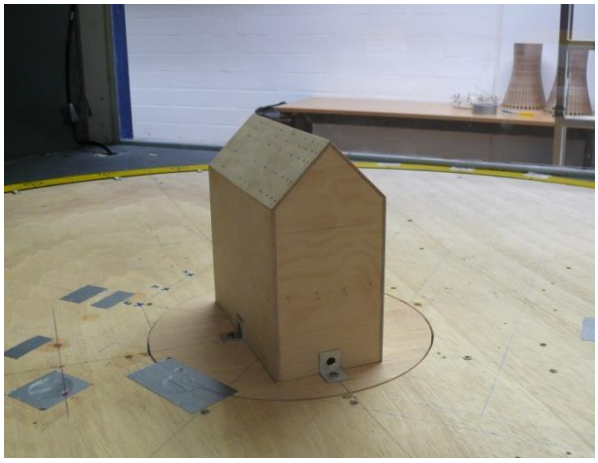

(a)

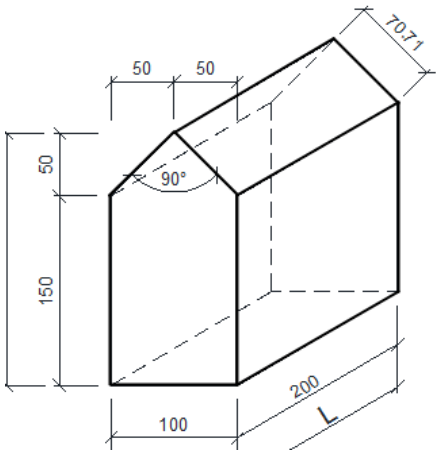

(b)

Figure 3 (a) Low-rise building mounted in the wind tunnel (b) dimensions of the low-rise model

2.4 Industrial building (hanger) with tilted roof

An industrial building with the tilted roof (hanger) placed at the rotating wind tunnel table is shown in Figure 4 (a). Figure 4(b) shows the dimensions of the used model.

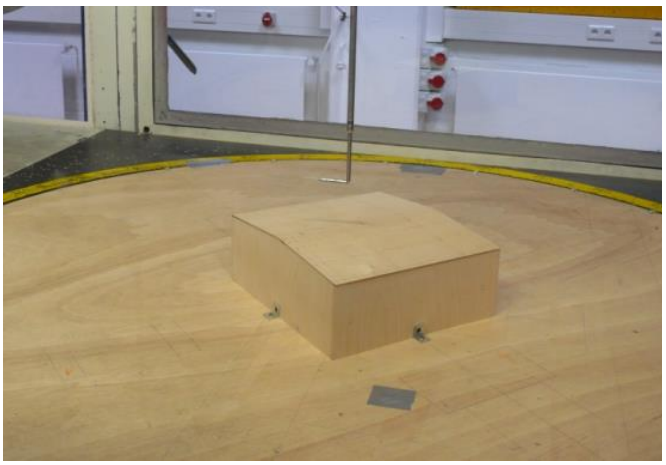

(a)

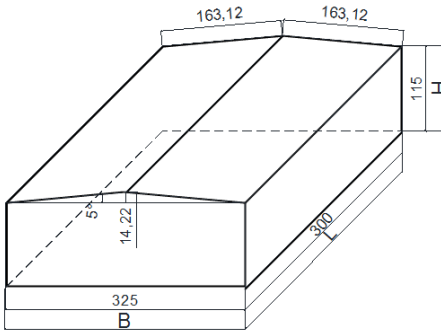

(b)

Figure 4 (a) Industrial building (Hanger) mounted in the wind tunnel, (b) dimensions of the industrial model

2.5 Interference configurations

The interference effect of the surrounding buildings was investigated in case of the high-rise building with the flat roof, high-rise building with the tilted roof and low-rise building with the tilted roof. All these configurations included the main building surrounded with four interfering buildings. Interfering buildings are represented as a copy of the main building with exactly same dimensions. The interference configuration mounted in the wind tunnel and used arrangement for the case of high-rise with flat and tilted roof are presented in Figure 5 (a) and Figure 5 (b) and in case of low-rise building in Figure 6 (a) and Figure 6 (b), respectively.

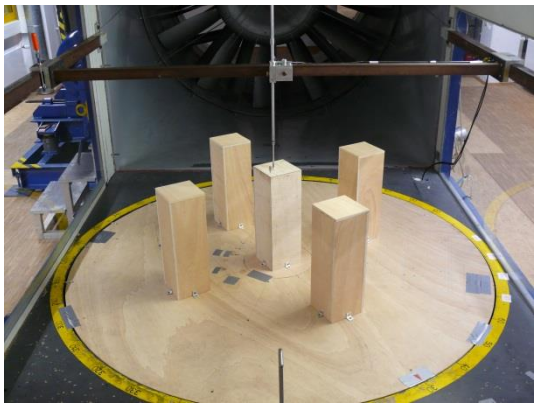

(a)

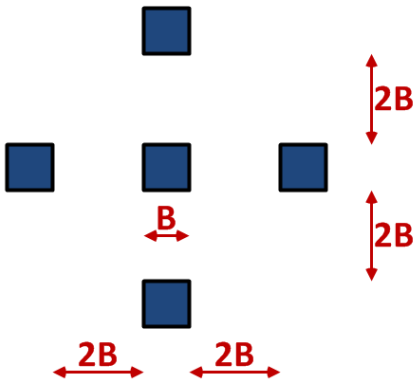

(b)

Figure 5 (a) Interference configuration of the high-rise building with flat roof mounted in the wind tunnel, (b) arrangement of the buildings in interference configuration of high-rise building

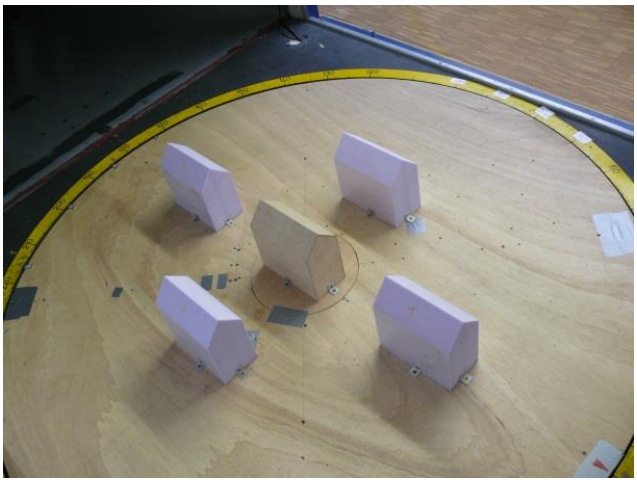

(a)

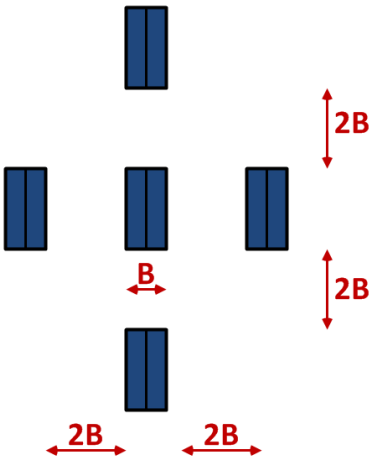

(b)

Figure 6 (a) Interference configuration of the low-rise building with tilted roof mounted in the wind tunnel, (b) arrangement of the buildings in interference configuration of low-rise building

3 Velocity measurements

Hot wire anemometry and measurements of mean dynamic pressure were used to measure velocity. A Prandtl tube mounted one meter upstream of the model was used to set the reference wind tunnel velocity for each test. Using the measured dynamic pressure, the mean wind speed is obtained applying Bernoulli equation.

The velocities above the roof of the above building shapes and configurations at different heights have been measured. For these measurements the necessary equipment consists of a hot wire anemometer, amplifier and analog/digital (A/D) converter. Anemometer consists of two cross wires with 5 μm in diameter and 1.2mm long that are suspended between two needle-shaped prongs (refer to Figure 7 (a)). These cross wires allow to measure two wind components. For these experiments, the velocity components in the stream-wise and vertical directions are chosen. No attempt has been made to measure the span-wise velocity component. Even though it is possible to place more hot-wire probes in the wind tunnel, in order to minimize the impact on the flow field, only one is used for all tests. The used sampling frequency was 2000 Hz.

The anemometer has been calibrated in a laminar flow in a calibration tunnel. The calibration establishes a relation between the output (in voltages) and the flow velocity. It is performed by exposing the probe to a set of known velocities (U) and corresponding voltages (E) are recorded. A fitting curve is estimated through the points (U,E) representing a transfer function, for each wire, that is used when converting data signal from voltages into velocities. The fitting curve which is adopted is a polynomial curve of 3rd order. The coefficients are calculated by fitting the data in the least-squares sense. Calibration curves used in this case are reported in Figure 8.

As an amplifier Multichannel CTA 54N80 by Dantec is used and all analog signals are converted to digital ones, using analog/digital (A/D) converter.

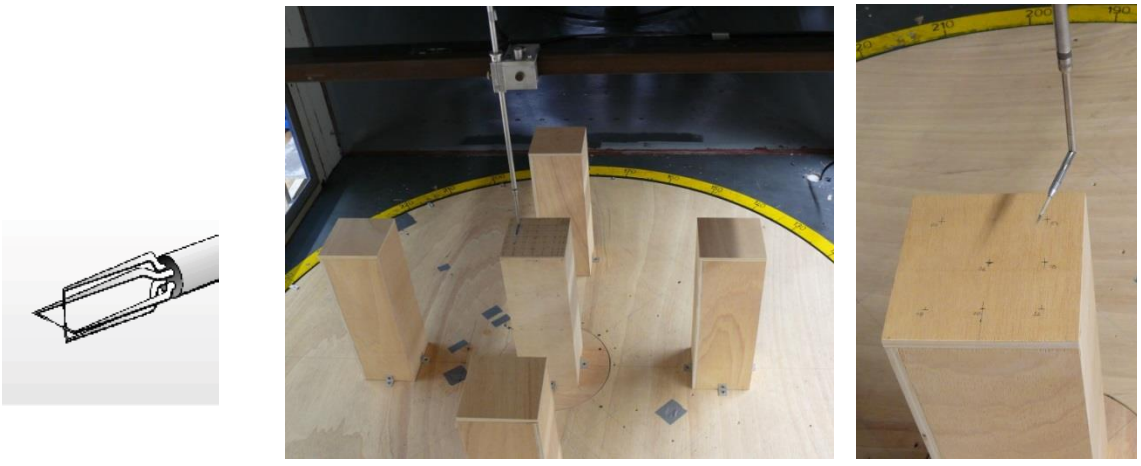

(a) (b) (c)

Figure 7 (a) Zoom at miniature wires (X array), (b) and (c) hot-wire during the measurements

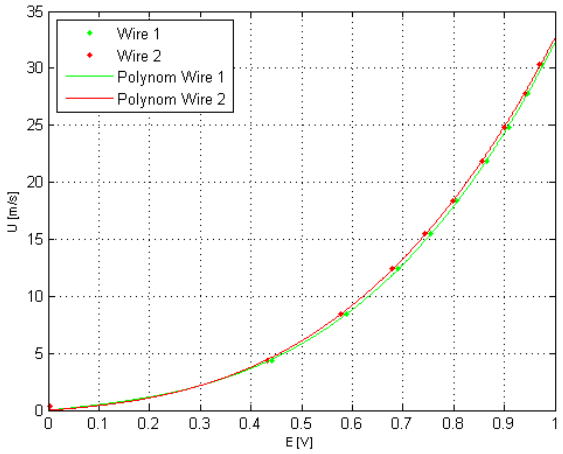

Figure 8 Calibration curves – wires 1 and 2 of used probe

4 Pressure measurements

Ninety pressure transducers are utilized to measure surface pressures on models placed mainly on the roof and the rings at certain heights of the buildings. For these pressure measurements the necessary equipment consists of pressure transducers (sensors), a tubing system, amplifiers and analog/digital (A/D) converters.

Two types of pressure transducers are used for this study:

- Honeywell 170 PC sensors
- AMSYS 5812-0001-D-B sensors.

Figure 9 (a) presents schematic representation of pressure sensor of type Honeywell where two chambers separated by one piezoresistant membrane can be seen. When the membrane is loaded with a pressure difference from the chambers, a deformation arises, which is associated with the change in the resistance in the piezoresistors. Both applied sensor types (Honeywell and AMSYS) are working by the same principle, by measuring differential voltage, and in this manner measuring differential pressures. In this particular case of measurements, the pressure difference is established as a difference of pressures at the model surfaces and static pressure of the Prandtl tube.

The calibration establishes the pressure-voltage relations for each pressure sensor. For that purpose, a Betz manometer is used, allowing loading the sensors with a known pressure. This way the link between the measured voltage and known pressure is established. For these measurements these relationships are acquired: for Honeywell sensors 5mbar corresponds to 5V and for AMSYS sensors 5mbar corresponds to 1V.

Due to the narrow spaces in the model (refer to Figure 10 (b)) the placement of the pressure sensors directly at the model surfaces is not possible, thus tubing system must be taken into account. Therefore, added acceleration response of the tubing system must be checked and if exists, eliminated. Identification of these undesirable effects is done by comparing the response spectrum of the measured signal when the tubes are used with the signal when tubes are not used, i.e. when the sensor is applied directly on the surface of a model. The later is considered to be the right measurement. Influence of these effects is captured with the transfer function of those pressure tubes and this residual influence on the pressure measurements is corrected by the application of a digital filter to the measured data using a MATLAB routine.

The amplifiers for the Honeywell pressure sensors are external and independent from each other. On the other hand, the amplifiers of the pressure sensors AMSYS are incorporated within the pressure cells. All analog signals are then converted to digital ones, using analog/digital (A/D) converters. The pressures are scanned with the sampling rate of 1000Hz in a sample-and-hold modus, which produces simultaneous sampling of pressures. The software used for recording is SBench 5.0.

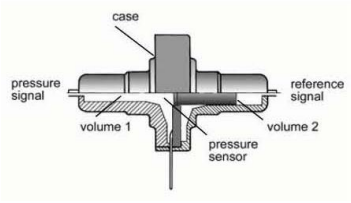

(a) (b) (c)

Figure 9 (a) Schematic representation of pressure sensor Honeywell 170 PC, (b) and (c) pressure cells

.

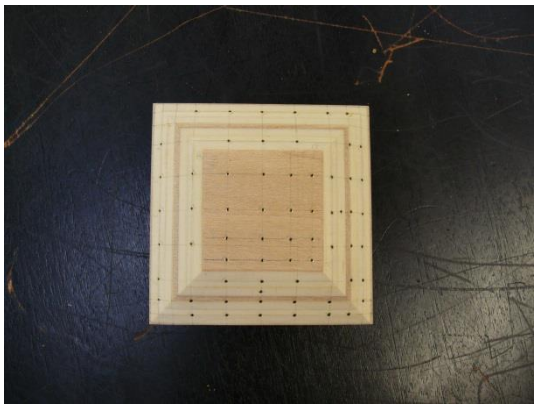

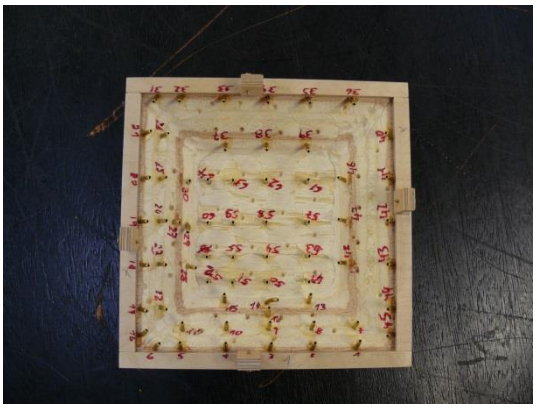

(a) (b)

Figure 10 Arrangement of the pressure taps on the tilted roof (a) top view and (b) view from inside of the model

5 Some results of the velocity measurements

Figure 11 shows profiles of the measured normalized mean stream-wise velocity and the turbulence intensity above the center of the high-rise building for wind direction of 0°. Measured profiles from two configurations, flow around the isolated building and when surrounded by interference buildings are shown. Wind tunnel results related to the isolated building are presented as averaged values out of three subsequent measurements. On the other hand, the measured stream-wise velocities related to the building surrounded by interference buildings are obtained out of a single measurement set. Therefore slight scatter can be observed related to the uncertainty of the measurement set-up. Nevertheless, the differences in curve trends, corresponding to the interference effect, can be observed. More detail analysis of the flow related to these two configurations is presented in Appendix B where the validated CFD results are presented. Reference velocity was measured using Prandtl tube placed 1m in front of the model at the height of 0.4m.

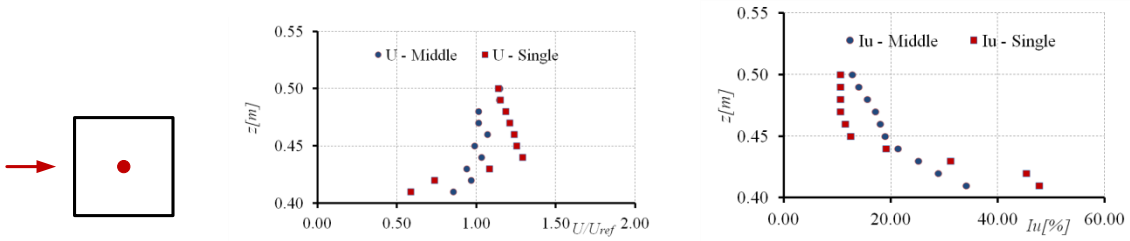

(a) (b) (c)

Figure 11 Wind flow profiles over the center of the single high-rise building (marked as 'Single') and center of the high-rise surrounded by interference buildings (marked as 'Middle'): (a) angle of flow attack, (b) normalized stream-wise velocity and (c) turbulence intensity

Figure 12 (b) and Figure 12 (c) present profiles of the measured normalized mean stream-wise velocity and the turbulence intensity above the center of the low-rise building investigated in isolations, respectively, for wind direction marked in Figure 12 (a). The results are obtained out of a single measurement set. More detailed analysis of the flow field is presented in Appendix C through validated results of CFD analysis.

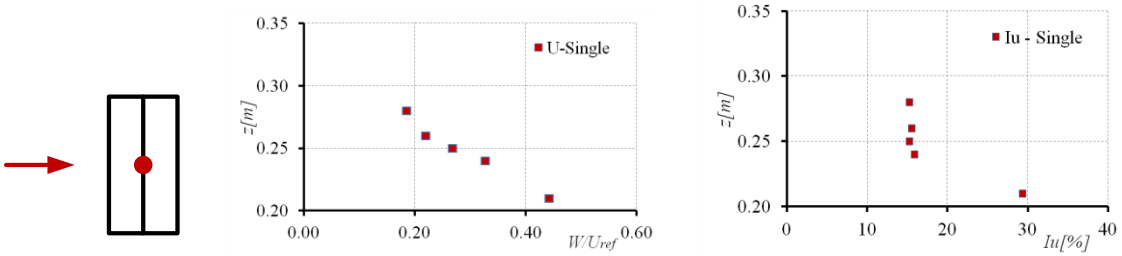

(a) (b) (c)

Figure 12 Wind flow profiles over the center of the single low-rise building: (a) angle of flow attack, (b) normalized stream-wise velocity and (c) turbulence intensity

In Figure 13 profiles of the measured normalized mean stream-wise velocity and the turbulence intensity above the center of the industrial building are presented for wind direction marked in Figure 13 (a). The presented results are obtained out of a single measurement set.

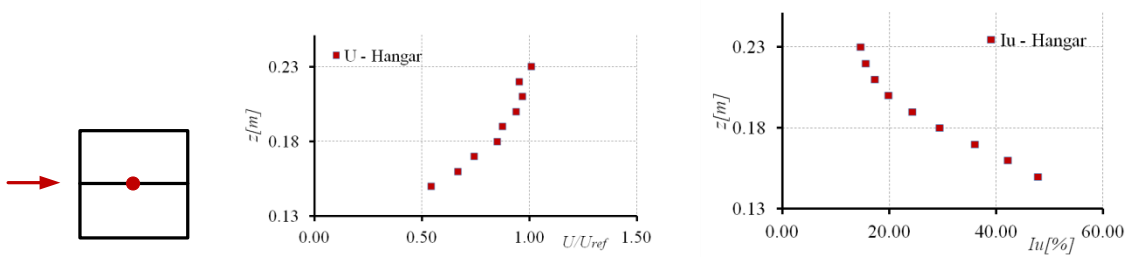

(a) (b) (c)

Figure 13 Wind flow profiles over the center of the industrial building: (a) angle of flow attack, (b) normalized stream-wise velocity and (c) turbulence intensity

More velocity results are shown in the attached papers.

6 Some results of the pressure measurements

Figure 14 shows measured distributions of the pressure coefficient over the central line at the roof top of the high-rise building for both considered cases, i.e. isolated building and when surrounded by interfering buildings. Again, more details of the corresponding flow fields can be found in Appendix B.

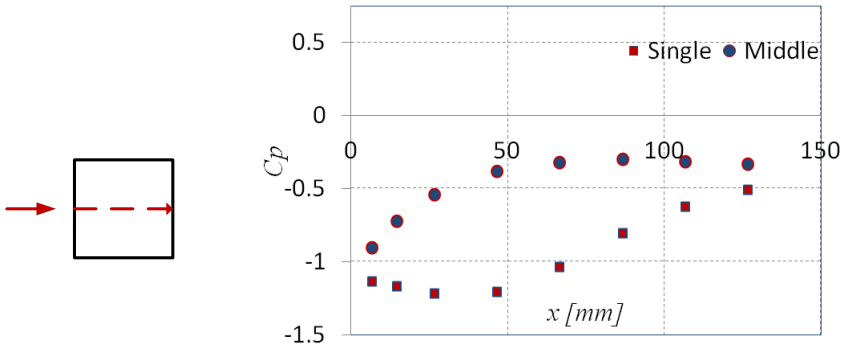

(a) (b)

Figure 14 (a) Angle of flow attack and central line (a) pressure coefficient distributions over the central line of the flat roof of the single high-rise building (marked as 'Single') and high-rise surrounded by interference buildings (marked as 'Middle')

Figure 15 shows the comparison of the measured distributions of the pressure coefficient over the central line at the tilted roof of low-rise building for both considered cases, i.e. isolated building and when surrounded by interfering buildings. It is noticeable that the windward side is changing the sign under the interference effect, from pressure to suction (Appendix C).

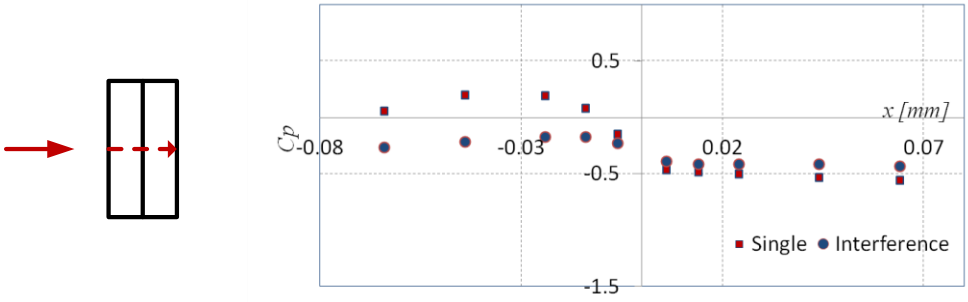

(a) (b)

Figure 15 (a) Angle of flow attack and central line (a) pressure coefficient distributions over the over the central line of the tilted roof of the single low-rise building (marked as 'Single') and low-rise surrounded by interference buildings (marked as 'Middle')

Figure 16 shows the distribution of the pressure coefficient over the ring at ¾ height of the high-rise building with the flat roof.

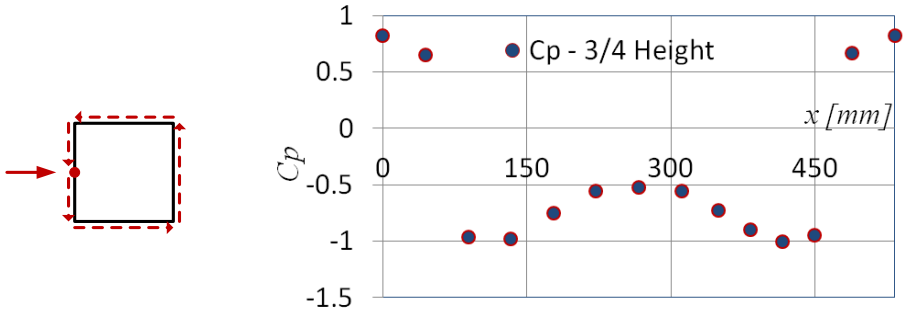

(a) (b)

Figure 16 (a) Angle of flow attack and the ring (a) pressure coefficient distributions over the ring at the ¾ of the total height of the high-rise building with the flat roof

More pressure results are in the attached papers.

Appendix A (Paper 1)

The above roof flow of a high-rise building for wind energy extraction; wind tunnel and numerical investigations

Hassan Hemida[1], Anina Šarkić[2], Rüdiger Höffer[3]
[1]School of Civil Eng., University of Birmingham, B152TT, UK
[2]Institute of Numerical Analyses and the Theory of Structures, University of Belgrade, Serbia
[3]Windingenieurwesen und Strömungsmechanik, Faculty for Civil and Environmental Engineering, Ruhr-University Bochum, Germany

Emails: h.hemida@bham.ac.uk, sarkicanina@gmail.com, Ruediger.Hoeffer@ruhr-uni-bochum.de

KEY WORDS: High-rise buildings; Wind Energy; wind tunnel experiment, LES, RANS

Abstract

In order to increase wind energy harvesting from urban environment, the wind behavior around high-rise buildings need to be fully understood. In this paper, both wind tunnel experiments and numerical modelling of the flow around a high-rise building with a height to width ratio of 3:1 were performed to investigate the wind distribution on the above roof flow. The building was mounted in an environmental boundary layer resembling that of the built environment. Two shapes of the roof of the building were investigated; flat and tilted roofs. Four different wind angles, with respect to the side of the high-rise building, were investigated experimentally; 0, 15, 30, and 45 degrees. Computational fluid dynamics using the SST-$k\omega$ RANS simulations were made for all the cases. In order to provide an in depth description of the flow around the building a detailed computation using large-eddy simulation was performed.

Introduction

Wind energy is harvesting since the existence of human being. Wind mills have been used to extract water from deep wells and in agriculture purposes. Since the discovery of electricity, wind turbines have been used to convert the wind energy into electricity and with the continuous rise of fuel prices, increase in carbon emissions and reduction of fusel fuel, wind energy has received considerable attentions as alternative and cheap energy source. Although the production of wind energy is predominantly from on-shore and off-shore wind farms, there are many difficulties associated with these technologies. For off-shore wind farms, these are related to the large cost of transmitting the energy to the costumers, foundation of wind energy system, structural fatigue due to the interactions between waves, winds and structure of the wind energy system, difficulties in maintenance, corrosion of the structure due to the salinity of the water, and many others. For on-shore wind farms, the issues are related to use of land, visual effect, effect on wild life, expensive maintenance and public resistance that made some countries to ban construction of new on-shore wind farms. To overcome some of these problems and issues and to promote the use of green energy from renewable resources, there is a strong trend in the European Union (EU) of promoting harvesting wind energy from built environment. This is evidenced by the recently awarded EU projects; COST action "TU1304" [1] and the H2020 ITN project "AEOLUS4FUTURE" [2]. The main aim of the first is to investigate the possibility of harvesting wind energy from urban environment and for the second is to transfer the established expertise from the on-shore and off-shore wind farms to the built environment. This is also supported by the Feed-in Tariff (FIT), a payment to people generating their own electricity from renewable sources, implemented by a number of EU governments, such as that implemented by the UK government in 2012. However, there are a number of issues associated with installing wind turbines in an urban environment, such as reduction in efficiency, noise, vibration, visual impact and many others that make social acceptance to these types of technology difficult. The efficiency of wind energy system in urban environment is related to the reduced wind

velocity and thus the amount of energy that can be harvesting. Also, the high turbulence intensity of the atmospheric boundary layer in urban environments decreases the turbine efficiency, increases noise and vibration and reduces life time of the wind energy device. Thus, more research is needed to investigate the best location on the roof of a high-rise building to mount a wind turbine, at which the wind velocity and turbulence are appropriate for wind energy harvesting.
The work of this paper has been undertaken as a part of a Short Term Scientific Mission of the COST Action "TU1304" to measure the flow around high-rise buildings for the purpose of wind energy harvesting. The main aim is to measure wind velocity at different locations in the above roof flow of a high-rise building. The building's height to width ratio is 3:1. Four different wind directions (angles), with respect to the side of the building, have been considered; 0^o, 15^o, 30^o and 45^o. These measurement data are considered as a base for validations of any further computational fluid dynamic (CFD) simulations. Surface pressure has been also measured to give an extra validation for the CFD investigations. Numerical simulations of the flow around the high-rise building have been made for all the wind angles using the Reynolds Averaged Navier Stocks (RANS) SST $k\omega$ model. In addition to the RANS simulations, a detailed simulation using the large-eddy simulation (LES) approach has been made for the flow around the building. In addition to validating the CFD, the wind velocities obtained from the wind tunnel test have been analyzed at the four mentioned wind angles and the turbulence statistics were calculated.

High-rise building model

Two 1:300 scale models of the high-rise building have been used; one with a flat roof and the other with a tilted roof as shown in Figures 1(a) and 1(b), respectively. As shown in Figure 1(a), the height of the building is denoted by *H* (400 mm) and the width by *B* (133.3 mm). The height to width ratio of the building is *H:B*=3:1.

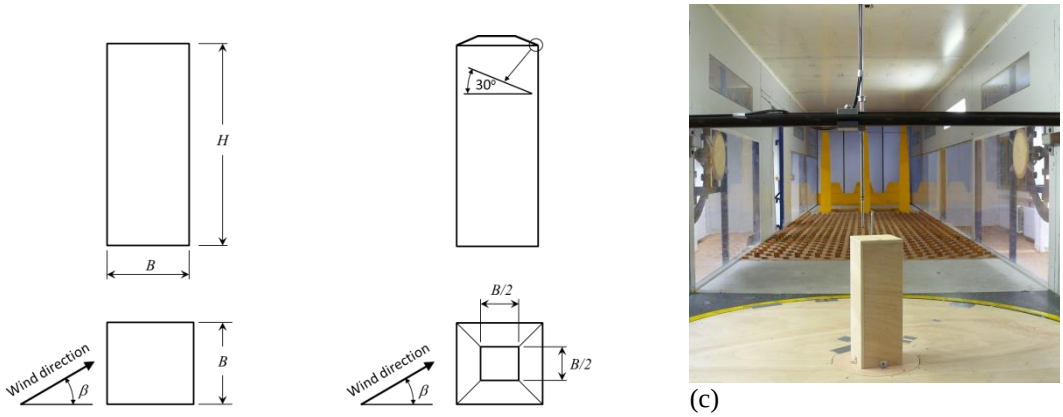

(a) (b) (c)

Figure 5 High-rise building model used in the investigation, (a) with flat roof, (b) with a tilted roof, and (c) when mounted in the wind tunnel.

Wind tunnel Experiments

The experiments have been conducted in the atmospheric boundary-layer wind-tunnel of the Ruhr-University Bochum, Germany. The wind tunnel has a cross section of 1.6 m x 1.8 m and a test section length of 9.4 m. Figure 1(c) shows the wooden model mounted on a rotating table in the wind tunnel. A two velocity components hot wire anemometer has been used to measure the velocity components in the stream-wise and vertical directions. No attempt has been made to measure the span-wise velocity component. The sampling frequency of the hot wire used was 2000 Hz. The anemometer has been calibrated in a laminar flow in a calibration tunnel. The atmospheric boundary layer has been simulated using a castellated barrier, turbulent generators and the roughness elements (cascaded small cubes of edge length 3.6 cm and 1.6 cm, respectively) as shown in Figure 1 (c). In addition to the velocity measurements, the surface pressure has been obtained at different locations to give extra data for the CFD validation. The pressure sensors are connected to the bores in the wooden model by optimized pressure

tubes with a length of about 0.9 m. Reference velocity was measured using Prandtl tube placed 1m in front of the model at the height corresponding to the height of the model.

Numerical Simulation

Two types of CFD approaches have been used in the current investigations; the RANS SST kω and large-eddy simulation (LES) using the standard Smagorinsky model. The wind tunnel velocity profile and turbulence intensity have been measured above the smooth floor at 1m distance from the roughness elements (refer to Figure 1 (c)).

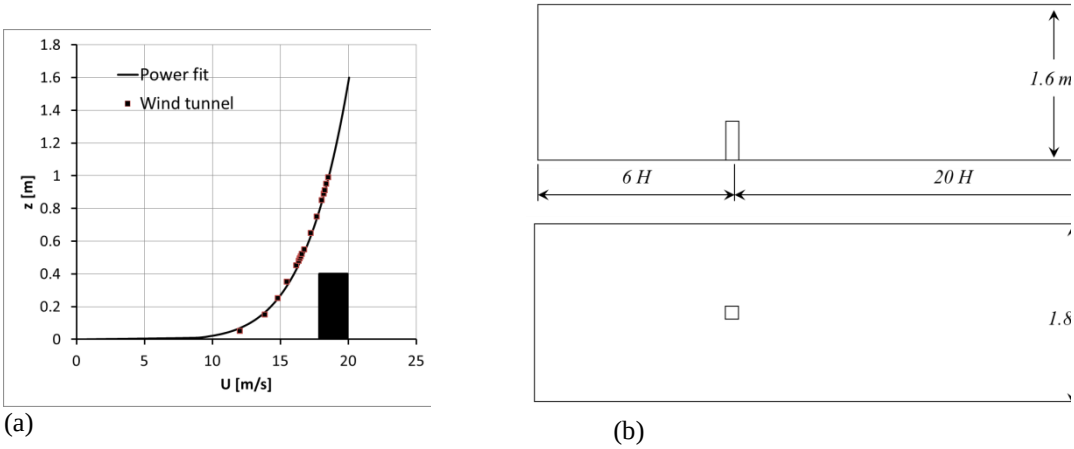

Figure 6. Computational details; (a) inlet velocity profile and (b) computational domain.

The mean inlet wind profile after the roughness elements is shown in Figure 2(a). This mean wind profile and turbulence intensity have been used as inlet boundary conditions of the RANS and LES simulations. For LES, two computations with different number of nodes have been used to investigate the mesh dependency for the two building models; coarse and fine meshes consist of 4m and 14m cells (Figure 3), respectively. All the RANS computations have been performed using the coarse mesh (Figure 3 (a)). The dimensions of the computational domain are similar to the cross section of the wind tunnel. The downstream distance between the exit plane and the model has been extended to ensure that there is no significant effect of the exit zero-pressure boundary condition on the results. Dimension of the computational domain is shown in Figure 3(b). A no-slip boundary condition has been used on the walls of the wind tunnel and the building.

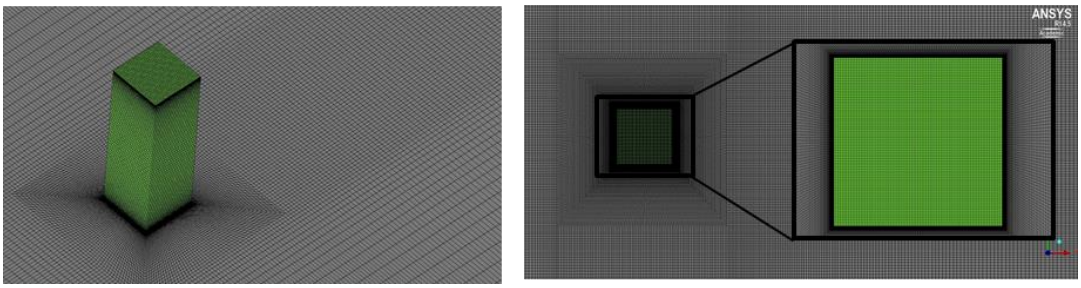

Figure 7 Surface mesh, (a) coarse mesh, (b) fine mesh distribution.

In order to investigate the effect of the inlet boundary conditions on the results, one LES simulation, including castellated barrier, turbulent generators and the rows of roughness elements generating similar instantaneous wind field ahead of the model as in the wind tunnel has been performed (Figure 4).

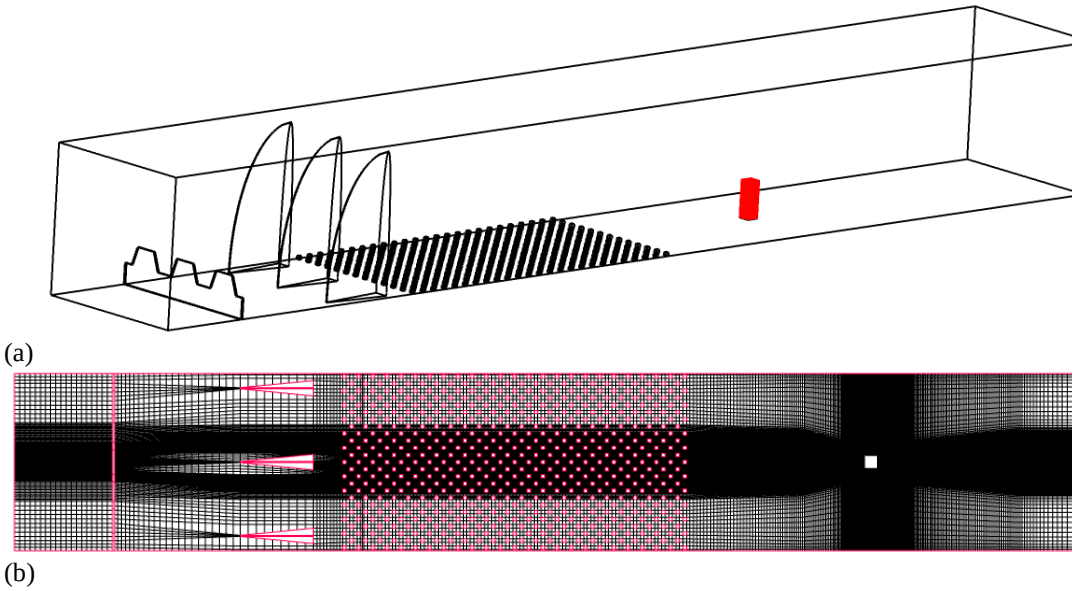

Figure 8 LES domain and coarse mesh distribution.

Results

Figure 5 shows measured mean stream-wise and vertical component of the velocity above the center of the high rise building for wind direction of 0°. The presented wind tunnel results are averaged values out of three subsequent measurements. The computed mean stream-wise velocity using RANS approach shows the same trend as in the measurements, jet under predicting the peak value. On the other hand, computed mean vertical velocity show over prediction compared to the measurement results. Similar deviation of the mean measured and RANS simulated vertical velocity over the cube are documented in [3]. These observations indicate a certain deviation of the measured and simulated flow field.
As observed in Figure 5 (c) measured turbulence intensity decreases with the height. Therefore, the region with high turbulence intensity (over 30%) is directly above the roof (up to 3cm) possibly indicating reverse flow region. Here the velocity vector falls outside the opening angle of the sensor [4]. Therefore, due to the lack of anemometer to detect the correct direction of the approaching stream-wise flow measured mean velocities in this region must be considered with caution and cannot be used for quantitative validation. Validated numerical results could provide clearer understanding of this region.

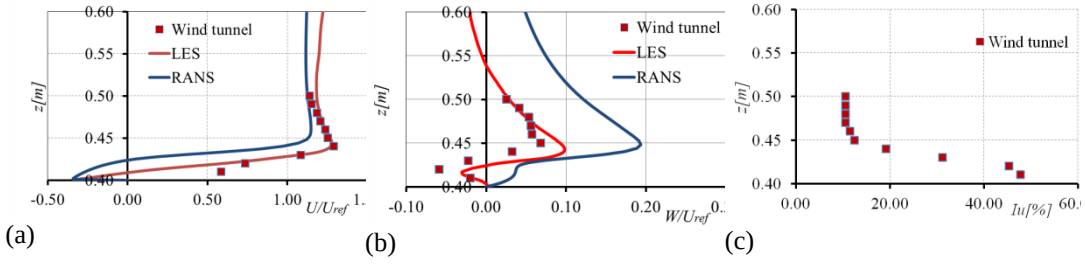

Figure 9 Wind flow profiles over the center of the high rise building, comparison of the present CDF simulations with the experiment: (a) normalized stream-wise velocity, (b) normalized vertical velocity and (c) turbulence intensity.

Figure 6 (a) shows the comparison of the measured and simulated distribution of the pressure coefficient over the central line at the roof top of the high rise building. It can be observed that RANS approach failed to provide correct prediction of this suction area. Namely, this area is related to a massive separated flow above the roof without the reattachment at the top as it is shown at Figure 5 (b). It is interesting to mention that similar result is obtained when LES simulation is performed using the same inlet boundary conditions as in case of RANS.

On the other hand, LES simulation that is simulating the approaching flow in the same manner as in the wind tunnel (Figure 2 (c)) shows good agreement of the predicted suction area and the wind tunnel results at the top of the building. Figure 5 (a) shows averaged LES flow field over the top of the building, with the qualitatively different pattern as observed in case of RANS simulations. Namely, the reattachment of the flow can be observed in the vicinity of the leeward edge. Therefore it can be concluded that the wind characteristics in the above roof flow are strongly dependent on the surrounding environment, highlighting the importance of the inlet boundary conditions. Figure 7 shows the surface oil-like print on the surface of the building demonstrating the regions of separation and reattachment.

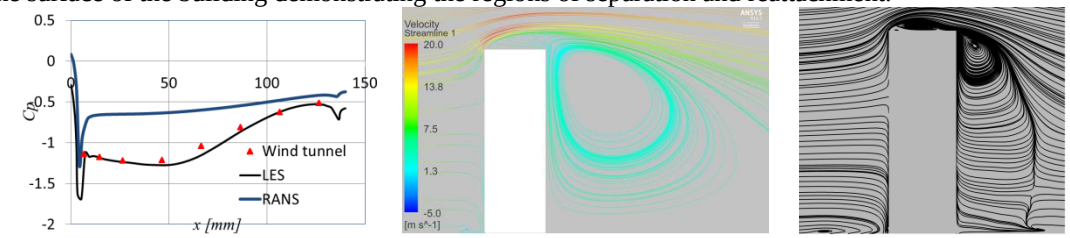

(a) (b) (c)

Figure 10 (a) Pressure coefficient distribution over the central line of the flat roof of the high rise building; Streamlines of the velocity flow field around the high-rise building with flat roof: RANS - SST $k\omega$ results (b) and LES results with similar boundary layer as in the wind tunnel.

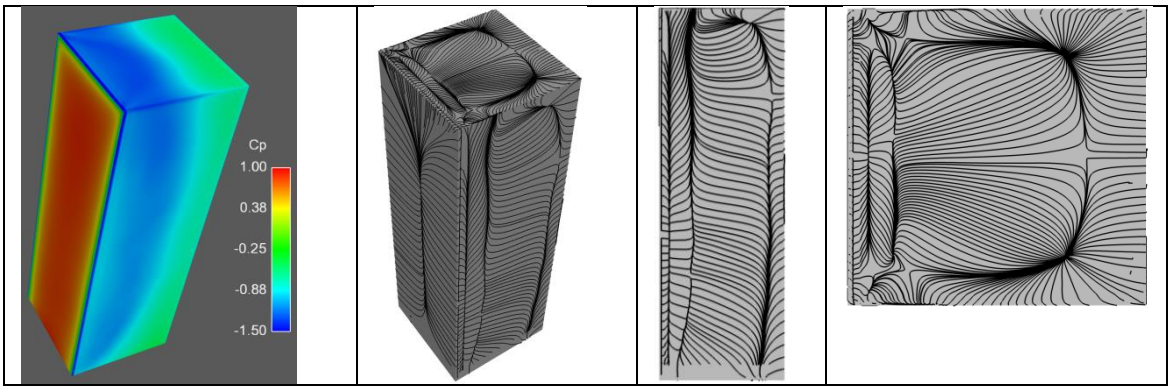

Figure 11 Cp and pathlines on the surface of the building

All the results from the different methods and at different wind angles will be presented in the final paper.

References

WINERCOST, Online http://www.cost.eu/COST_Actions/tud/Actions/TU1304

AEOLUS4FUTURE http://www.uc.pt/fctuc/dec/investigacao/areascientificas1/projeto/mecestru

L. Ledo, P.B. Kosasih, P. Cooper (2011): Roof mounting site analysis for micro-wind turbines, In: Renewable Energy, 36 (5), 1379-1391

Dantec Dynamics (2004): MiniCTA Anemometer How to get started - a quick Guide. Skovlunde and Denmark.

Appendix B (Paper 2)

Interference effect of high-rise buildings for wind energy extraction; wind tunnel and numerical investigations

Hassan Hemida[1], Anina Šarkić[2], Rüdiger Höffer[3]
[1]School of Civil Eng., University of Birmingham, B152TT, UK
[2]Institute of Numerical Analyses and the Theory of Structures, University of Belgrade, Serbia
[3]Windingenieurwesen und Strömungsmechanik, Faculty for Civil and Environmental Engineering, Ruhr-University Bochum, Germany

Emails: h.hemida@bham.ac.uk, sarkicanina@gmail.com, Ruediger.Hoeffer@ruhr-uni-bochum.de

KEY WORDS: High-rise buildings; Wind Energy; wind tunnel experiment, LES, RANS.

Abstract

In order to increase wind energy harvesting from urban environment, the wind behavior around high-rise buildings and the effect of the surrounding buildings need to be fully understood. In this paper, both wind tunnel experiments and numerical simulations of the flow around a high-rise building with a height to width ration of 3:1 surrounded by fours similar buildings were performed to investigate the interference effect on the above roof flow. The buildings were mounted in an environmental boundary layer resembling that of a built environment. Two shapes of the roof of the principle building were investigated; flat and tilted roofs. Four different wind angles, with respect to the side of the high-rise building, were investigated experimentally; 0, 15, 30, and 45 degrees. Computational fluid dynamics using the SST-$k\omega$ RANS simulations were made for all the cases and an in depth investigation of the flow around the buildings configurations at 0 degree was performed using large-eddy simulation.

Introduction

It is known that the greenhouse effect is the most harmful environmental problem facing the world nowadays. Carbon dioxide (CO2) is the one of the main greenhouse gases that the world leaders, politicians and scientists are working hard to set rules in order to reduce its emission. For instance, the UK government set a plan in which by 2050 the CO2 emission should be reduced by 80% of that of 1990 [1]. One of the several options available to help achieving this target is to move towards the renewable green energy and encouraging the zero-carbon houses. The latter is a building that uses renewable energy and does not contribute to any CO2 emissions. It is well known that wind carries considerable amount of energy that can produce enough electricity for the entire human needs if no other source of energy is in use. However, nowadays only less than 0.1% of this energy is in use [2]. There are quite a number of issues with harvesting wind energy such noise, vibrations, visual and environmental impact. In order to avoid some of these problems, wind farms are installed off-shore as wind speed is higher and also to overcome the problem of noise and to reduce the impact on environment. This however, comes with other drawbacks such as the increased cost and problems associated with off-shore foundations and impact on see life. Recently, harvesting wind energy from urban environment has received considerable attentions from both researchers and decision makers and some of the European countries implemented the Feed-in Tariff (FIT) to encourage the public to explore the possibility of for instance installing wind turbine on the roof of their houses [3]. There are a number of issues associated with harvesting wind energy from urban environment all tend to reduce the public acceptance of such technology. The most important issues are the noise, vibration, efficiency of the wind energy system, safety and visual impact. The lower efficiency of wind turbines in urban environment is related to the low wind speed as a result of surface roughness such as buildings and trees. Also the interference effect of the surrounding buildings might affect the wind speed and the turbulence in the wind approaching the location of the wind turbine. However, the effect of the neighboring buildings on both wind speed and turbulence intensity in the above roof flow is not fully understood and needs more investigations. Therefore the aim of this paper is

to give an improved understanding of the flow above a roof of high-rise building surrounded by four similar buildings and subjected to atmospheric winds with different angles; 0, 15^o, 30^o and 45^o.

The results are based on both wind tunnel experiments and numerical simulations using two different approaches; steady Reynolds Averaged Navier Stocks (RANS) and large-eddy simulations (LES). The velocity profiles at the above roof flow have been measured experimentally at all the wind yaw angles. The numerical simulations of the flow around the high-rise building, single and surrounded by four similar buildings, have been made for all the wind angles using the RANS approach with SST-$k\omega$ turbulence model. In addition to the RANS simulations, a detailed simulation using the large-eddy simulation (LES) approach has been made for the flow around the building at 0^o wind angle. The work of this paper has been undertaken as a part of a Short Term Scientific Mission of the COST Action "TU1304" to measure the flow around high-rise buildings for the purpose of wind energy harvesting.

High-rise building model

Two 1:300 scale models of high-rise building are used as principle buildings; one with flat roof and the other is with tilted roof as shown in Figures 1(a) and 1(b), respectively. As shown in Figure 1(a), the height of the building is denoted by *H* (400 mm) and the width by *B* (133.3 mm). The ratio of the height to width is *H/B*=3/1.

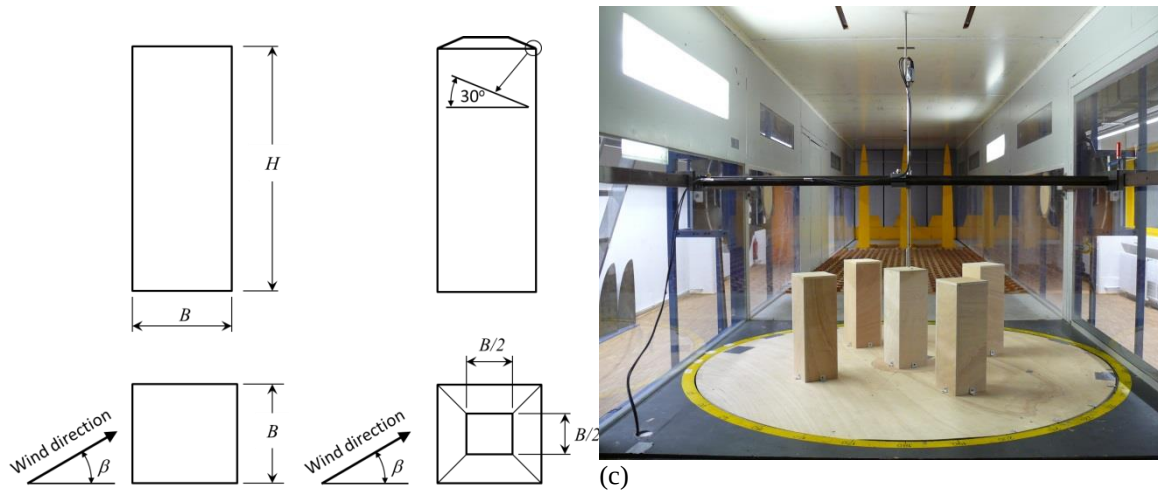

Figure 12 Investigated buildings. (a) Building with flat roof, (b) building with tilted roof and (c) the principle building surrounded by the interference buildings in the wind tunnel.

The four interfering buildings are a copy of the principle building with flat roof with exactly the same dimensions. The principle building and the interference ones were arranged as shown in Figure 2 (a).

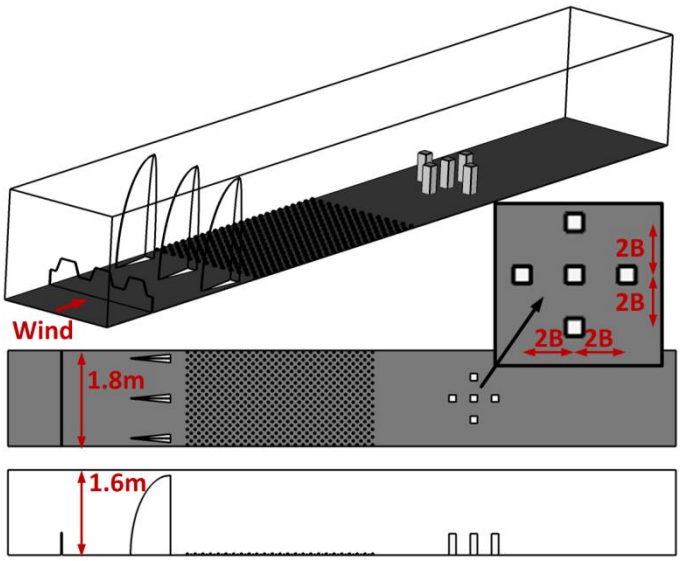

(a)

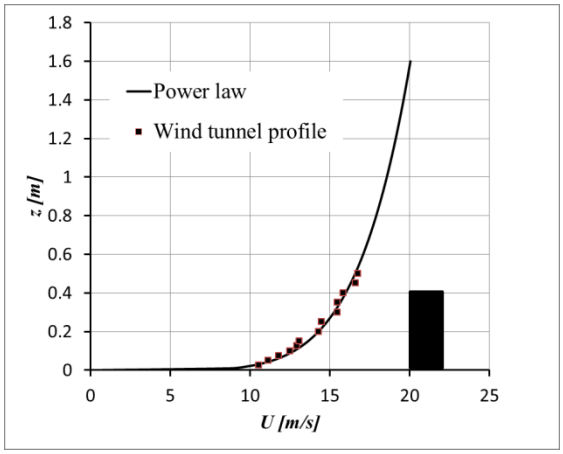

(b)

Figure 13 (a) RANS domain and arrangement of principle and interference buildings, (b) wind tunnel and CFD velocity profiles.

Wind tunnel Experiments

The experiments have been conducted in the atmospheric boundary-layer wind-tunnel of the Ruhr-University Bochum, Germany. The wind tunnel has a cross section of 1.6 m x 1.8 m and a test section length of 9.4 m. Two arrangements were tested: one is a single wooden model mounted in the middle of the rotating table and the other model is surrounded by four wooden interfering buildings (refer to Figure 1(c)). A two velocity components hot wire anemometer has been used to measure the velocity components in the stream-wise and vertical directions. No attempt has been made to measure the span-wise velocity component. The sampling frequency of the hot wire used was 2000 Hz. The anemometer has been calibrated in a laminar flow in a calibration tunnel. The atmospheric boundary layer has been simulated using a castellated barrier, turbulent generators and the roughness elements (cascaded small cubes of edge length 3.6 cm and 1.6 cm, respectively) as shown in Figure 1 (c). In addition to the velocity measurements, the surface pressure has been obtained at different locations to give extra data for the CFD validation. The pressure sensors are connected to the bores in the wooden model by optimized pressure tubes with a length of about 0.9 m. Reference velocity was measured using Prandtl tube placed 1m in front of the model at the height corresponding to the height of the model.

Numerical Simulation

Two types of CFD approaches have been used in the current simulations; the RANS SST-$k\omega$ model and large-eddy simulation (LES) using the standard Smagorinsky model. Two types of computational domains have been used; one is similar to the test section of the wind tunnel in which the wind tunnel velocity profile and turbulence intensity have been measured above the smooth floor at 1m distance from the roughness elements (refer to Figure 1(c)) and one simulates the entire wind tunnel. The mean inlet wind profile after the roughness elements is shown in Figure 2(b). The former computational domain is used for the flow around the single building. The latter is used for RANS simulations in the case of principle building surrounded by interference buildings (group arrangement), including castellated barrier, turbulent generators and the rows of roughness elements generating similar wind field ahead of the model as in the wind tunnel has been performed. Dimensions of this computational domain are shown in Figure 2(a). The downstream distance has been extended to ensure that there is no significant effect of the exit zero-pressure boundary condition on the results. A no-slip boundary condition has been used on the walls of the wind tunnel and the buildings. For LES, two computations with different number of nodes have been used to investigate the mesh dependency for the two building models; coarse and fine meshes.

Results

Figure 3 shows profiles of the measured normalized mean stream-wise velocity and the turbulence intensity above the center of the high rise building for wind direction of 0°. Measured profiles from two configurations, flow around the principle building alone and when placed in a group arrangement, are compared with the corresponding RANS results. The computed mean stream-wise velocity over the single building using RANS approach shows the same trend as in the measurements, jet under predicting the peak value. These wind tunnel results are averaged values out of three subsequent measurements. On the other hand, the measured stream-wise velocities related to the principal building, placed in a group arrangement, are obtained out of a single measurement set. Therefore slight scatter can be observed related to the uncertainty of the measurement set-up. Nevertheless, in this case, general trend of the measured profile over the principle building can be observed. When compared with the corresponding RANS results a certain change in the slope of the stream-wise velocity component is observed.

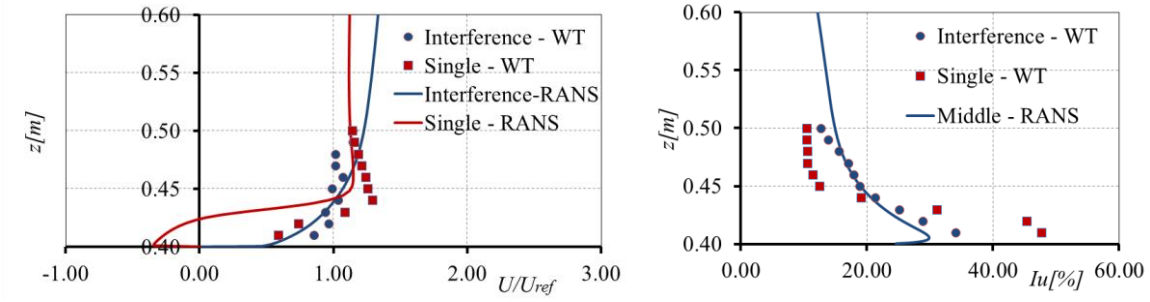

(a) (b)

Figure 14 Wind flow profiles over the center of the single high rise building (marked as 'Single') and center of the high rise surrounded by interference buildings (marked as 'Middle'), comparison of the present RANS simulations with the experiment: (a) normalized stream-wise velocity, (b) turbulence intensity.

Figure 4(a) shows the comparison of the measured and simulated distributions of the pressure coefficient over the central line at the roof top of the high rise building for both considered cases, i.e. principal building alone and in a group arrangement. It can be observed that in the case of the flow around the principal building alone, RANS approach did not provide correct prediction of the suction area at the top of the building. A massive separated flow without the reattachment above the roof is simulated by RANS (refer to Figure 4(b)). Jet, the same trend of decreasing these suction values at the top of the principle building by placing it in group arrangement, is observed in RANS results as in the case of the measurements. Moreover, in the case of the principal building placed in a group arrangement, very good agreement is observed between numerical and experimental results.

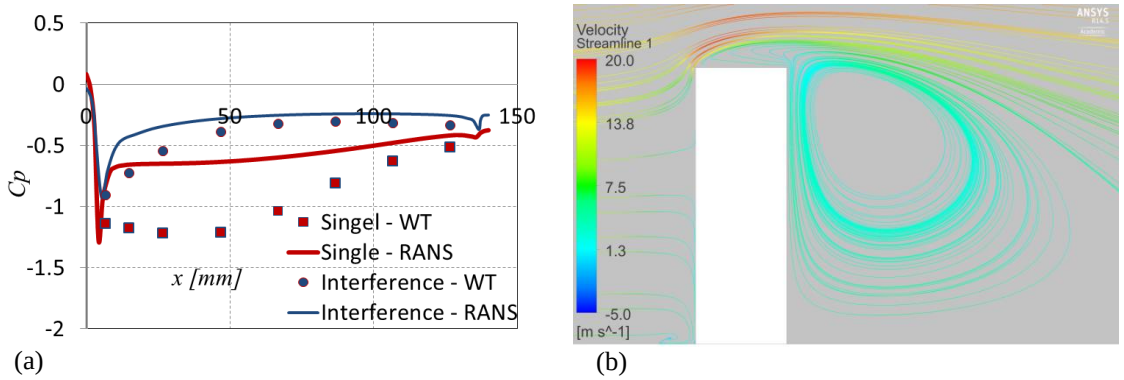

(a) (b)

Figure 4 (a) Pressure coefficient distribution over the over the central line of the flat roof of the single high rise building (marked as 'Single') and high rise building placed in group arrangement (marked as 'Middle'), comparison of the present RANS simulations with the experiment; (b) Streamlines of the velocity flow field around the high-rise building with flat roof: RANS results

The main reason for this change in suction trends over the principle building in two arrangements can be observed in Figure 5(a). Here the flow pattern above the principle building is presented when it is surrounded by interference buildings. Namely, incoming flow separates from the top of the upstream building and generates a shear flow that affects, as well, the flow over the principal building. This effect can be also seen by comparing measured turbulence intensity profiles over the center of the principle building alone and when placed in the group arrangement (refer to Figure 3(b)). It can be observed that turbulence intensity over the building in group arrangement is not experiencing the same sharp drop just above the region very close to the roof. Thus, at higher heights higher values of measured turbulence intensities are observed when compared with the case of the single building. Figure 5(b) shows velocity streamlines around the buildings.

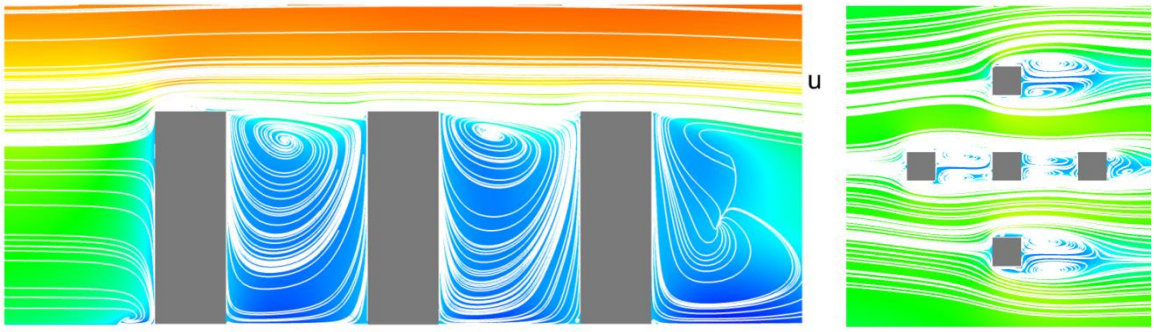

(a) (b)

Figure 5 Flow around the principle and interfering buildings.

All the results from the different methods and at different wind angles will be presented in the final paper.

References

ESRC, How people use and ‘misuse’ buildings. Swindon: Econ. & Soc. Res. Counc, 2009.

WWEA, small wind; world report, 2014 Online: www.small-wind.org.

H. Hemida., Large-eddy simulation of the above roof flow of a high-rise building for micro-wind turbines, 11th UK Conference on Wind Engineering, Birmingham, 2014

Appendix C (Paper 3)

Experimental and numerical investigations of the flow above a tilted roof house for urban wind energy harvesting

Anina Šarkić[1], Hassan Hemida[2], Rüdiger Höffer [3]
[1] Institute of Numerical Analyses and the Theory of Structures, University of Belgrade, Serbia
[2]School of Civil Eng., University of Birmingham, B152TT, UK
[3] Windingenieurwesen und Strömungsmechanik, Faculty for Civil and Environmental Engineering, Ruhr-University Bochum, Germany

Emails: sarkicanina@gmail.com, h.hemida@bham.ac.uk, Ruediger.Hoeffer@ruhr-uni-bochum.de

KEY WORDS: Urban environment; Wind Energy; wind tunnel experiment, LES, RANS.

Abstract

In this paper, the best location for installing a micro wind turbine on a roof of a house has been investigated using wind tunnel and numerical simulations. The house model is a 1/75th scale with tilted roof. The wind behavior around the house was obtained at three different wind angles: 0, 45 and 90 degrees relative to the direction of the house longest edge. The measurements of the wind velocity above the building were carried out in an atmospheric boundary layer wind tunnel. Computational fluid dynamics using the RANS SST-kω simulations were also made for all the wind angles and an in depth investigation of the flow around the house at 0 degree wind angle was performed using large-eddy simulation. The velocity profile of the flow above the roof of the house was measured at different heights and used to validate the numerical modelling. The computational fluid dynamic results were analyzed and revealed the best location of a wind turbine to be installed. In addition, both wind tunnel experiments and numerical simulations of the flow around the tilted house surrounded by four similar houses were performed to investigate the interference effect on the above roof flow.

Introduction

Worldwide, existing buildings consume about 40% of the world's energy and are responsible for approximately the same percentage of global carbon emissions (UNEP, 2007). Thus there is a strong need to reduce the carbon foot print of houses through the use of green and environmental friendly source of energy. Among others, wind and solar are the most feasible renewable energy sources that can allow buildings to be energy producers rather than consumers and thus reduce the CO2 emissions. However, the amount of solar energy that could be extracted on a roof of a house is very small compared to the available wind energy around the building. Still, there are a number of issues related to wind energy systems, such as noise, efficiency of the wind energy system, safety and cost, that need to be resolved before this energy harvesting technology can be promoted in urban areas.

Due to the large roughness size, urban environment is characterized by low wind speed compared to the rural areas. In order to maximize the wind extraction from the urban environment, the wind turbine is recommended to be installed on the houses' roof. However, the wind velocity is not the same above the roof of a house and thus to maximize the wind extraction the wind turbine should be installed at the spot with the highest wind speed and lowest turbulence intensity as possible. The latter is to minimize noise, vibration and fatigue and to increase the overall wind turbine efficiency.

Many researchers have been attracted to study the flow around buildings, using wind tunnel experiments [1] and computational techniques [2], [3] and [4]. Most of these investigations are focused on the flow around a standard shapes, cubes or prism with very little studies on the flow around non-standard building shapes. Moreover, most of the studies of the flow around buildings have been carried out for the purpose of wind loading and limited studies looked at the wind energy harvesting. Also the interference effect has been studied by researchers for the purpose of wind loading. An example of this is the work of Kim et. al., [1] in 2010. They investigated the interference effect on local peak pressures between two buildings. This is done by using detailed wind tunnel experiments which included investigation of the

effects of relative heights, various locations and wind directions of an interfering building on interference effects for local peak pressures.

The work of this paper is thus to investigate the flow around a house with a tilted roof and subjected to atmospheric wind. The main aim is to reveal the flow characteristic around the house in order to estimate the best location for installing a micro wind turbine on the roof of the house. As the wind continually changes its direction, one location could be best for one wind direction but not for the others. In order to assess this, velocity profile above the roof of the house at three wind directions have been investigated; 0, 45 and 90 degrees measured from the direction of the maximum length of the building. Surface pressure has been also measured to give an extra validation for the CFD investigations. The flow has been obtained at the three wind angles using computational fluid dynamics (CFD) and the results have been validated using wind tunnel experiments. Also the wind tunnel signals have been used to reveal the turbulence intensity. In order to accurately visualize the flow around the building, a detailed computation using large-eddy simulation (LES) has been performed. Also the surrounding buildings might have a great effect on the speed and the turbulence intensity of the wind approaching the location of the wind turbine, but this effect is not properly quantified. Therefore, additional aim of this paper is to give an improved understanding of the flow above a tilted house roof surrounded by four similar houses and subjected to atmospheric winds with different angles. The work of this paper has been undertaken as a part of a Short Term Scientific Mission of the COST Action "TU1304" to measure the flow around buildings for the purpose of wind energy harvesting.

House model

A 1/75th scale model of a tilted roof house is used as a principle building. Two configurations are studied: one isolated house and one in which the house (principle) is surrounded by four similar houses (interference houses). The dimensions of the principal house are given in Figure 1(a) and the inclination of the roof is 45°. The four interfering houses are a copy of the principle house with exactly the same dimensions. The principle house and the interference ones were arranged as shown in Figure 2 (a) and Figure 1(c).

(a) (b) (c)

Figure 15 (a) Dimensions of the tilted roof model, (b) tilted roof model mounted on the rotating table in the wind tunnel and (c) the principle house surrounded by the interference houses mounted in the wind tunnel.

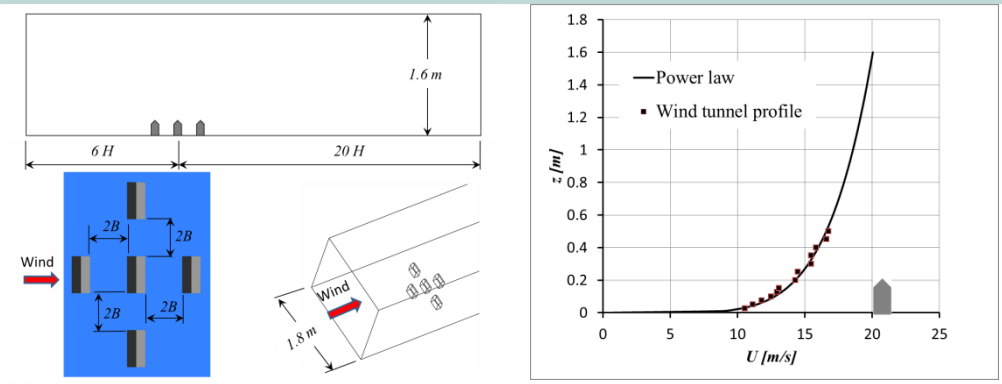

(a) (b)

Figure 16 (a) RANS domain and arrangement of the houses in the wind tunnel and in numerical simulation, (b) wind tunnel and CFD velocity profiles.

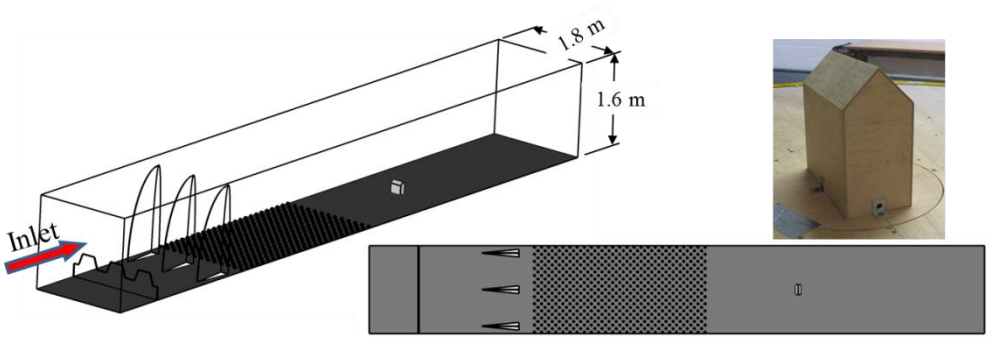

Figure 17 RANS domain for the single tilted house configuration simulating the entire wind tunnel.

Wind tunnel Experiments

The experiments have been conducted in the atmospheric boundary-layer wind-tunnel of the Ruhr-University Bochum, Germany. The wind tunnel has a cross section of 1.6 m x 1.8 m and a test section length of 9.4 m. Figure 1(b) shows the wooden model mounted on a rotating table in the wind tunnel. A two-velocity components hot wire anemometer has been used to measure the velocity components in the stream-wise and vertical directions. No attempt has been made to measure the span-wise velocity component. The sampling frequency of the hot wire was 2000 Hz. The anemometer has been calibrated in a laminar flow in a calibration tunnel. The atmospheric boundary layer has been simulated using a castellated barrier, turbulent generators and the roughness elements (cascaded small cubes of edge length 3.6 cm and 1.6 cm, respectively) as shown in Figure 1 (b). In addition to the velocity measurements, the surface pressure has been obtained at different locations to give extra data for the CFD validation. The pressure sensors are connected to the bores in the wooden model by pressure tubes with a length of about 0.6m. Reference velocity was measured using Prandtl tube placed 1m in front of the model at the height of 0.4m.

Numerical Simulation

Two types of CFD approaches have been used in the current simulations; the RANS SST-$k\omega$ model and large-eddy simulation (LES) using the standard Smagorinsky model. Two types of computational domains have been used; one simulates the entire wind tunnel and the other is a smooth channel with a cross section similar to that of the test section of the wind tunnel in which the wind tunnel velocity profile and turbulence intensity, measured above the smooth floor at 1m distance from the roughness elements (refer to Figure 1(c)) were used as inlet boundary conditions. The mean inlet wind profile after the roughness elements is shown in Figure 2(b). The former computational domain is used for the flow around the single building including castellated barrier, turbulent generators and the rows of roughness

elements generating similar wind field ahead of the model as in the wind tunnel. Dimensions of this computational domain are shown in Figure 3 and details of corresponding mesh on Figure 4. The latter is used for RANS simulations in the case of principle house surrounded by interference houses (group arrangement). The computational domain and corresponding mesh are presented in Figure 2(a) and Figure 5, respectively. The downstream distance has been extended to ensure that there is no significant effect of the exit zero-pressure boundary condition on the results. A no-slip boundary condition has been used on the walls of the wind tunnel and the buildings. For LES, two computations with different number of nodes have been used to investigate the mesh dependency for the two building models; coarse and fine meshes.

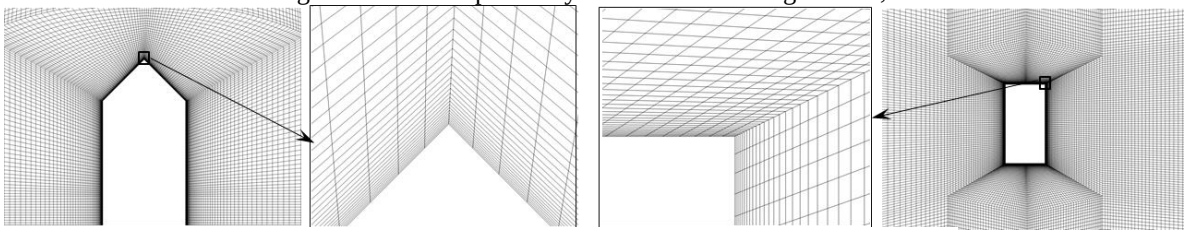

Figure 18 Mesh distributions around the single building configuration.

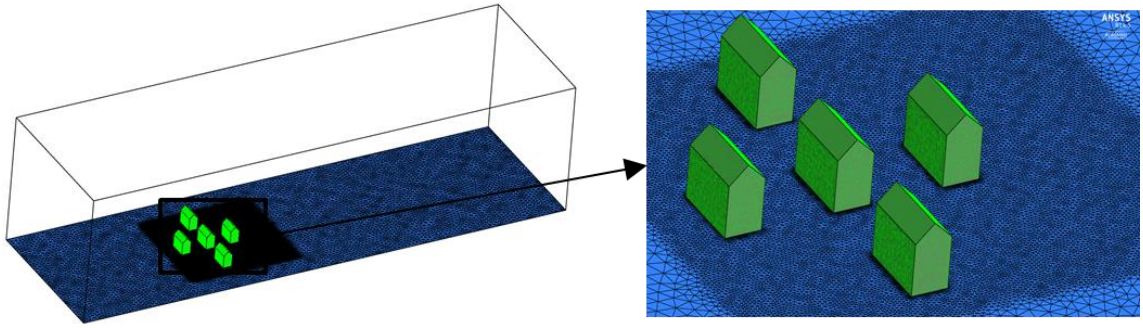

Figure 19 Mesh shape related to the configuration of principle house surrounded by interference houses (group arrangement).

Results

To validate the CFD methodology wind velocity over the centre of the single tilted roof house was simulated and compared to wind tunnel experiments. From Figure 6, it can be observed that the profiles from the computed normalized mean stream-wise and vertical velocity agree well with the measurements. Namely, as it can be observed in Figure 7(a), this profile is related to a start of a massive separated flow which is created in the area above the leeward part of the roof and behind the house. On contrary, Figure 7(b) presents the flow pattern above the principle house when it is surrounded by interference houses. In this case incoming flow separates from the roof of the upstream house and generates a shear flow that affects the flow over the principal house. The corresponding computed normalized mean stream-wise and vertical velocity profiles at the centre of the roof are included in Figure 6.

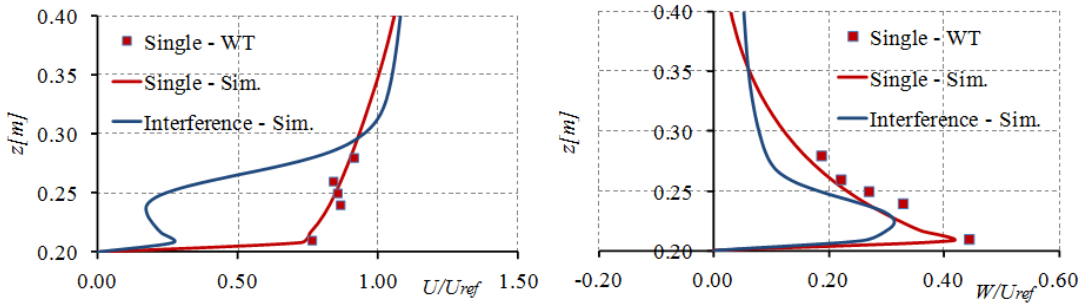

(a) (b)

Figure 6 Wind flow profiles over the centre of the single tilted roof house (marked as 'Single') and centre of the tilted roof house surrounded by interference houses (marked as 'Interference'), comparison of the present RANS simulations with the experiment: (a) normalized stream-wise velocity, (b) normalized vertical velocity.

Figure 8 shows the comparison of the measured and computed distributions of the pressure coefficient over the central line at the tilted roof for both considered cases, i.e. principal house alone and in the group arrangement. In the case of the single tilted house, the windward side is affected by pressure area and better prediction of the pressure coefficients is obtained. Main differences are obtained in leeward region, where RANS approach did not provide correct prediction of the suction area. Yet, the RANS results show the same trend of decreasing these suction values at the leeward side of the tilted roof of the principle house by placing it in group arrangement as in the case of the measurements. Moreover, by placing the principal building in the group arrangement, the change of pressure windward area into the suction area is simulated as well. This change is due to the different pattern of the incoming flow affected by the upwind house (Figure 7(b)).

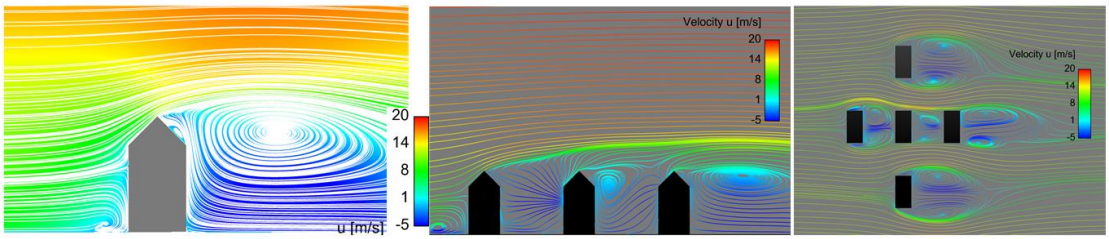

(a) (b) (c)

Figure 7 Flow around the principle house when it is treated alone (a) and surrounded by interfering houses (b) and (c).

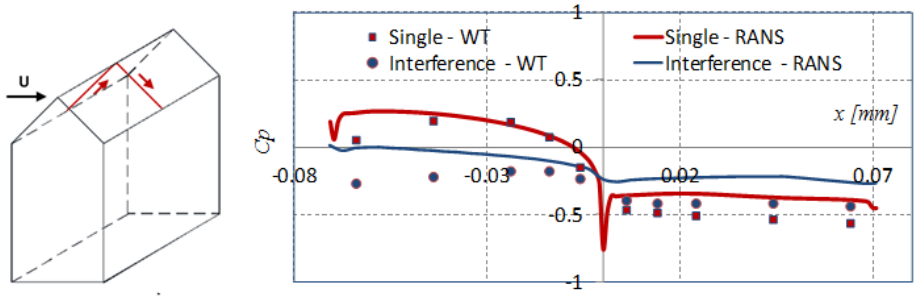

Figure 8 Pressure coefficient distribution over the central line of the tilted roof of the single house (marked as 'Single') and principal house placed in group arrangement (marked as 'Interference'), comparison of the present RANS simulations with the experiment.

All the results from the different methods and at different wind angles will be presented in the final paper.

References

[1] W. Kim, Y. Tamura, and A. Yoshida (2010): Interference effects on local peak on local peak pressures between two buildings, In: Journal of wind engineering and industrial aerodynamics, 90, 584-600.

[2] D. Ayhan, S. Saglam (2012): A technical review of building-mounted wind power systems and a sample simulation model, In: Renewable and sustainable energy reviews, 16, 1040-1049.

[3] H. Hemida: Large-eddy simulation of the above roof flow of a high-rise building for micro-wind turbines, 11th UK Conference on Wind Engineering, Birmingham, 2014

[4] L. Ledo, P.B. Kosasih, P. Cooper (2011): Roof mounting site analysis for micro-wind turbines, In: Renewable Energy, 36 (5), 1379-1391